

Polymer Communication

# The crystallization morphology and melting behavior of polymer crystals in nano-sized domains

Wei-Min Hou<sup>a</sup>, Jian-Jun Zhou<sup>a</sup>, Zhi-Hua Gan<sup>b</sup>, An-Chang Shi<sup>c</sup>,  
Chi-Ming Chan<sup>d</sup>, Lin Li<sup>a,\*</sup>

<sup>a</sup> State Key Laboratory of Polymer Physics and Chemistry, Institute of Chemistry, The Chinese Academy of Sciences, Beijing 100080, PR China

<sup>b</sup> The CAS Laboratory of Engineering Plastics, Institute of Chemistry, The Chinese Academy of Sciences, Beijing 100080, PR China

<sup>c</sup> Department of Physics and Astronomy, McMaster University, Hamilton, Ontario L8S 4M1, Canada

<sup>d</sup> Department of Chemical Engineering, Hong Kong University of Science and Technology, Hong Kong, PR China

Received 11 May 2007; received in revised form 13 June 2007; accepted 20 June 2007

Available online 28 June 2007

## Abstract

The crystallization morphology and the melting behavior of the phase-separating poly( $\epsilon$ -caprolactone) (PCL) and poly(ethylene oxide) (PEO) blends were studied using atomic force microscopy. Two blends consisting of PCL and PEO with weight ratios of 10/90 and 90/10 were prepared to form the isolated spherical domains by the phase-separating process. The results show that the melting temperatures of the PCL and PEO lamellae in the confined domains increased as the lamellar length increased, and the melting behavior of the PCL and PEO lamellae in the matrix and confined domains was also studied.

© 2007 Elsevier Ltd. All rights reserved.

**Keywords:** Polymer blend; Confined crystallization; Melting behavior

## 1. Introduction

Numerous studies on binary polymer blends can be found in the literature [1–17]. In particular, binary blends of two crystallizable polymers have a wide variety of interesting phase morphologies and complicated crystallization behavior [4–10]. The properties of the blends of two crystallizable polymers depend on the miscibility of the components as well as on their crystalline superstructures and phase morphologies. When a semi-crystalline polymer is finely dispersed in an immiscible matrix, isolated droplets of the semi-crystalline polymer of different sizes may form, providing opportunities to study the crystallization of the polymer in confined systems. Examples include the crystallization within the dispersed droplets in immiscible polymer blends [18–20], the

microphase-separated block copolymers [21–29] and the dewetting of ultrathin films [30–35]. Most previous studies focused on crystallization behaviors, such as the size-dependence of the nucleation and the crystallization rates. The melting behaviors of poly(ethylene oxide) (PEO) in the nano-sized spheres of a poly(butadiene-*b*-ethylene oxide) copolymer were studied by Reiter et al. using atomic force microscopy (AFM) [26]. They observed a distribution of melting temperatures across the individual PEO spheres. For example, the 12-nm PEO spheres melted at about 45 °C, which is about 20 °C lower than the PEO bulk melting temperature. They suggested that the difference in the melting temperature could be attributed to the different degrees of perfection of the crystals. Despite many previous studies, the influence of geometrical confinement on polymer crystal melting is not yet fully understood. In this study, we report the change in the melting temperature of lamellae of poly( $\epsilon$ -caprolactone) (PCL)/PEO blends crystallized in nano-sized confined domains by high-temperature AFM. The nano-sized domains in the blends

\* Corresponding author. Tel./fax: +86 10 8261 9830.

E-mail address: [lilin@iccas.ac.cn](mailto:lilin@iccas.ac.cn) (L. Li).

were obtained by controlling the blend composition and the phase-separating process.

## 2. Experimental section

Both PCL ( $\overline{M}_n = 8.0 \times 10^4 \text{ g mol}^{-1}$ ) and PEO ( $\overline{M}_w = 1.0 \times 10^5 \text{ g mol}^{-1}$ ) used in this study were purchased from Sigma–Aldrich Co. Solutions of the blends of PCL/PEO with weight ratios of 10/90 and 90/10 were prepared in chloroform. The blend solutions ( $10 \text{ mg ml}^{-1}$ ) were dropped on clean glass substrates at room temperature and dried under a vacuum for 24 h. The sample was melted at  $80^\circ\text{C}$  in a Linkam LTS350 hot stage and held at that temperature for 5 min, then quenched to the desired crystallization temperature, at which the samples were held for a specified time. The thickness of the films was around  $0.5 \mu\text{m}$ . The AFM observations were performed with a Nanoscope III MultiMode scanning probe microscope (Digital Instruments, Santa Barbara, California) equipped with a hot stage accessory. The detailed experimental conditions of high-temperature AFM can be found elsewhere in the literature [36,37]. The AFM images were obtained in the tapping mode using silicon tips (TESP, Digital Instruments) with a resonance frequency of approximately  $300 \text{ kHz}$  and a spring constant of about  $40 \text{ N m}^{-1}$ . Both the height and phase images were taken simultaneously.

## 3. Results and discussion

PCL and PEO are semi-crystalline polymers with bulk melting temperatures of about  $60$  and  $67^\circ\text{C}$ , respectively. In the bulk, neat PEO and PCL exhibit lamellar morphologies when crystallized at  $0^\circ\text{C}$  (cf. Fig. 1). The difference in the lamellar structures and lamellar thicknesses of PEO and PCL can be easily seen in the AFM phase images. As shown in Fig. 1a, a spherulite of PEO mainly consists of short edge-on lamellae with a wheat-like morphology. The average lamellar thickness was measured to be about  $14 \pm 2 \text{ nm}$ . Fig. 1b shows a spherulite of PCL, which consists of fibrillar bundles

that are made up of long and continuous edge-on lamellae. The average lamellar thickness is about  $9 \pm 2 \text{ nm}$  which was determined using AFM height images.

When a film of the PCL/PEO (10/90) blend was heated to  $80^\circ\text{C}$ , which is above the melting temperatures of both PCL and PEO, liquid–liquid phase separation occurred, as shown in Fig. 2a. The PEO formed the continuous matrix while the PCL was found in the dark isolated domains. Isolated PCL droplets, with sizes ranging from tens to hundreds of nanometers, were dispersed in the PEO matrix. The study of the PCL/PEO blends with a series of ratios suggested that the PEO became the dispersed phase when its weight fraction was lower than 50%.

After being crystallized at  $0^\circ\text{C}$  for 30 min, lamellar structures of the continuous PEO phase and the dispersed PCL phase developed, as shown in Fig. 2b. The PCL lamellae, which were crystallized in the isolated domains with diameters in tens to hundreds nanometers were confined by the PEO lamellae. The average PCL lamellar thickness, measured with the high-resolution AFM height images obtained at room temperature, is about 9, 10, 8,  $10 \pm 2 \text{ nm}$  in the domains with diameters of about 50, 110, 130 and  $150 \pm 5 \text{ nm}$ , respectively. It is worth noting that the average lamellar thickness in the different confined domains did not vary that much and was similar to that of the neat PCL lamellae. The lamellar thickness was found to be independent of the domain size because the PCL lamellae developed at the same degree of supercooling. However, the lengths of the PCL lamellae are very different even in the same domains. Taking the PCL domain marked with a circle in Fig. 2b as an example, the shortest and longest lamellar lengths are about 10 and 100 nm, respectively. Due to the confined space and the curved interface, the PCL lamellae with various lengths had to develop in confined domains. It is also interesting to note that the growth directions of the PCL lamellae differ even in neighboring domains, as indicated by the arrows in Fig. 2b, suggesting that the PCL domains are isolated from each other. The volume fraction of dispersed domains seems larger than 10%, suggesting that the phase

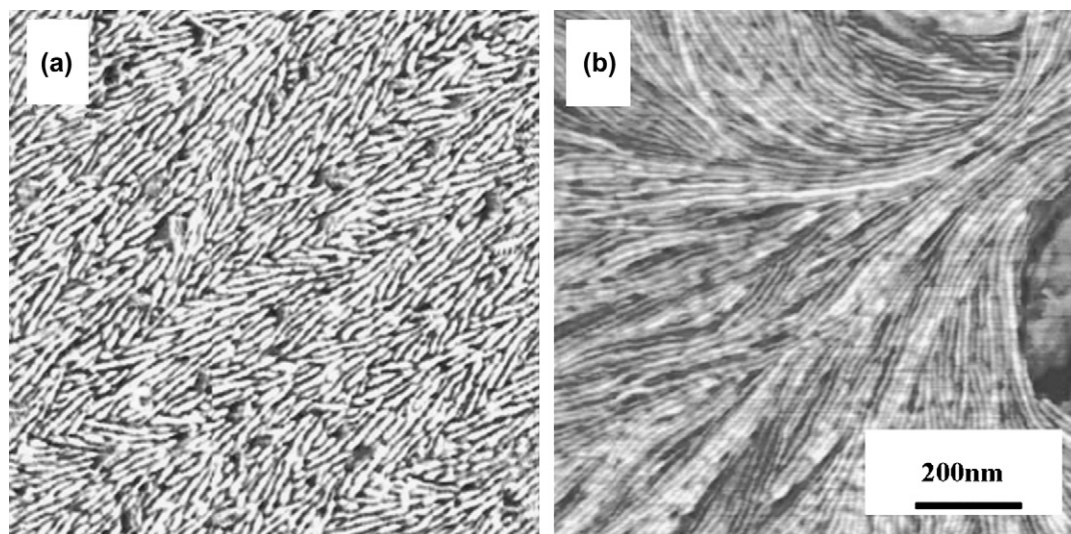


Fig. 1. The lamellar morphologies obtained by AFM phase imaging of (a) PEO and (b) PCL, crystallized at  $0^\circ\text{C}$  for 30 min.



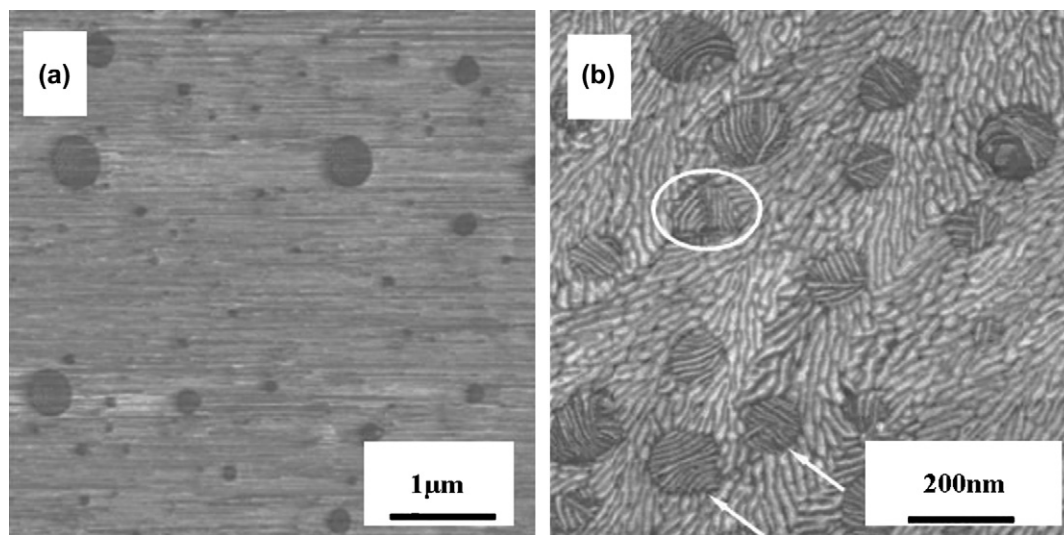


Fig. 2. AFM phase images of a PCL/PEO (10/90) blend: (a) annealed at 80 °C and (b) crystallized at 0 °C.

separation process may not fully develop or the PCL and PEO may be partially miscible in the amorphous phase, possibly due to the suppressing of the ongoing phase separation by crystallization [38–41]. The detailed experiments exploring the nucleation occurred in the individual domains independently are currently underway and will be reported in a forthcoming paper.

We now turn to the study of the melting of the PCL lamellae in the PCL/PEO (10/90) blend. Because the melting temperature of PEO is about 7 °C higher than that of PCL, the melting of the PCL lamellae occurs in the confined environment provided by the PEO lamellar matrix. Therefore, the PCL/PEO (10/90) blend is an ideal system for studying the influence of confinement on polymer lamellar melting.

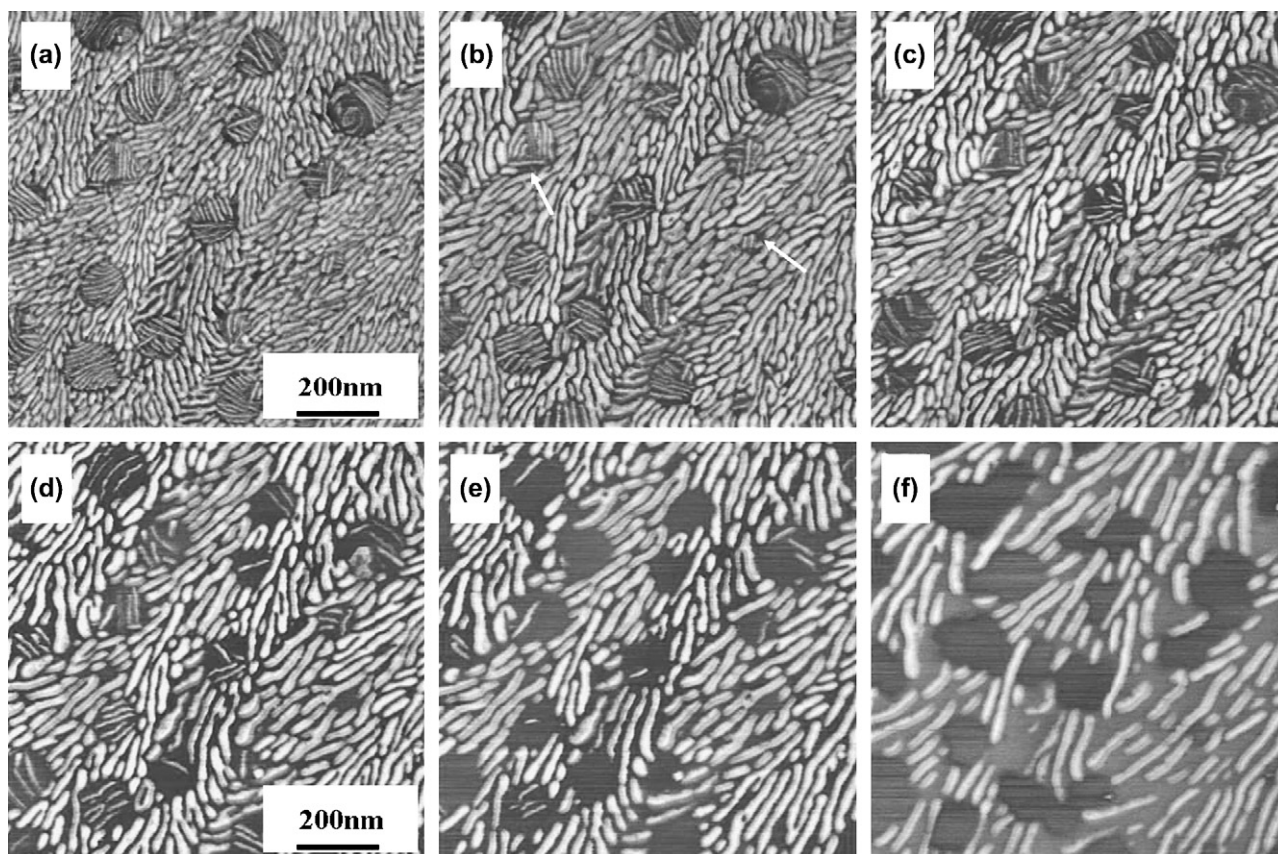


Fig. 3. The melting behavior of the PCL lamellae in isolated domains with different sizes followed by a series of AFM phase images at elevated temperatures: (a) 30, (b) 50, (c) 54, (d) 56, (e) 58, and (f) 60 °C. The time interval between two consecutive images is about 12 min.

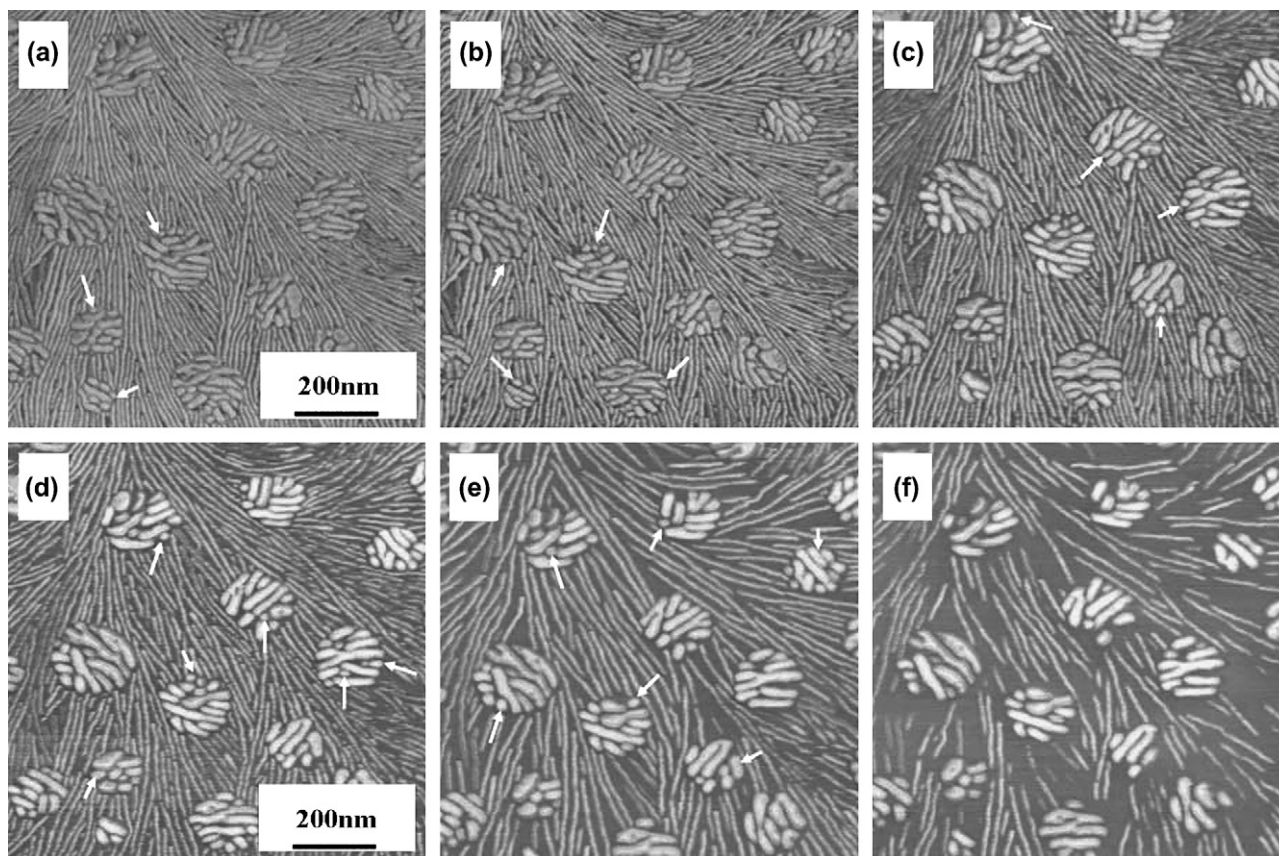


Fig. 4. The melting behavior of the PEO lamellae in isolated domains with different sizes followed by a series of AFM phase images at elevated temperatures: (a) 30, (b) 45, (c) 52, (d) 54, (e) 56, and (f) 58 °C. The time interval between two consecutive images is about 12 min.

The melting process can be monitored in real time using a hot-stage, high-resolution AFM at different temperatures. Fig. 3 presents a series of AFM phase images showing the melting process at elevated temperatures. When the temperature was increased to 50 °C, the shortest PCL lamellae of about 10 nm in length in some of domains melted first, while the longer PCL lamellae remained crystalline, as indicated by the arrows in Fig. 3b. At 54 °C, the PCL lamellae with lengths of about 20–50 nm melted, as shown in Fig. 3c, while the PCL lamellae with the lengths longer than 70 nm stayed solid. With a further increase in the temperature to 56 °C, the melting of the longer PCL lamellae was observed, as shown in Fig. 3d. At 58 °C, most of the PCL lamellae melted except for a few very long ones, as shown in Fig. 3e. All PCL lamellae melted at 60 °C (cf. Fig. 3f). In addition, the PEO lamellae, which were present in the continuous phase, became thicker, possibly due to reorganization during the heating [42–44]. In summary, our results show that the average PCL lamellar thickness in domains of different sizes was approximately constant and similar to that of the neat PCL. However, the melting temperature of the PCL lamellae depended strongly on their lengths, suggesting that the PCL lamellae with different lengths developed in variously sized confined domains had different thermal stabilities. The difference in the melting temperature may be due to the different degrees of perfection of the PCL lamellae that had to develop in the confined space and had to adapt the curved interface of the domains, which

may trap more defects in the lamellae. It is also reasonable to postulate that the shorter the PCL lamellae, the higher the ratio of defects (such as chain end groups, loose loop, lateral and chain folding surfaces) per unit length of the PCL lamellae developed in the confined space. Therefore, the melting of the short lamellae usually occurred at a low temperature during annealing.

To gain a more comprehensive understanding of the melting behavior of the lamellae developed in a confined environment, a PCL/PEO (90/10) blend was also studied. Fig. 4 shows a series of AFM phase images of the melting process of the PEO and PCL lamellae in a PCL/PEO (90/10) blend. In this blend, the PEO is the dispersed phase because it is the minor component. The long PCL lamellae developed in the continuous matrix. The melting behavior of the PCL lamellae in the continuous phase was observed using AFM. When the temperature was increased to 54 °C (cf. Fig. 4d), many long edge-on PCL lamellae in the matrix became discontinuous and the length of the melted parts is around 20–40 nm. Upon a further increase in temperature to 56 °C, the melting of the PCL lamellae became more prominent. The length of the melted parts is around 80–100 nm. Moreover, the PCL lamellae with the length less than 100 nm have been melted, as shown in Fig. 4e. After the temperature reached 58 °C, most of the PCL lamellae melted into pieces (cf. Fig. 4f.) and the length of the melted parts is above hundreds of nanometers. Our *in situ* AFM observations clearly indicate that the melting



behavior of the PCL lamellae developed in the continuous phase is similar to those developed in the confined domains (cf. Fig. 3e). For the PCL lamellae crystallized in the matrix, the degree of perfection of different parts of a single lamella and of different lamellae is not the same even though they have similar appearances and are developed at the same degree of supercooling. Considering the inhomogeneity of the polymer chains including end groups and chain conformations, parts of the lamella may contain more defects such as loops and end groups trapped in the lattice. Therefore, these parts of the PCL lamellae are relatively less stable and initial melting may occur at a relatively lower annealing temperature. When the annealing temperature was increased, the PCL lamellae continually melted from the initial molten parts, probably without undergoing recrystallization process, and the length of the melted parts increased. Similarly, the ratio of defects per unit lamellar length of the short one should be much larger than that of the long one, the PCL lamellae with different lengths crystallized in variously sized confined domains had different thermal stabilities. The shorter the PCL lamellae, the lower the melting temperature.

The similar melting behavior of the PEO lamellae crystallized in the matrix and in the nano-sized domains can be observed, as shown in Figs. 3 and 4, respectively. As the temperature was increased from 30 to 45 °C, the morphological changes occurred in the spherical PEO domains. The short lamellae of about 10 nm in length, which were located near the PEO domain boundary, started to melt. They were marked with arrows in Fig. 4a and b. When the temperature was increased to 52 °C, the PEO lamellae around 30 nm in length began to melt, as indicated by arrows. Moreover, the thickening of the PEO lamellae in the continuous matrix and differently sized domains became very obvious at annealing temperature around 50–52 °C, as shown in Figs. 3b and 4c. A careful comparison of Fig. 4a and c shows that the number of PEO lamellae in the same domain also decreased significantly. It suggested that the reorganization of the PEO lamellae initially occurred at the temperature around 50–52 °C. Upon a further increase in temperature to 56 °C, the PEO lamellae located in the middle and near the boundary of the domains melted and some melted PEO lamellar pieces rejoined together and reorganized to the thicker ones. When the temperature reached 58 °C, most of the shorter PEO lamellae melted except for the longer ones located in the middle of the domains. Our results suggested that the melting temperatures of the PEO lamellae also depended strongly on their lengths, indicating that the PEO lamellae with different lengths developed in the continuous matrix and variously sized confined domains had the similar thermal stabilities with the PCL lamellae. The shorter the PEO lamellae, the lower the melting and reorganization temperatures.

#### 4. Conclusion

In summary, for the PCL lamellae crystallized in the continuous matrix, our results suggest that the thermal stability is not uniform within a single lamella and among different

lamellae even if they are developed at the same degree of supercooling. For the PCL and PEO lamellae crystallized in the confined nano-sized domains, the thermal stability of the lamellae is strongly affected by the lamellar length. Although all lamellae in a domain have similar thicknesses, the shorter lamellae melt at lower temperatures. Moreover, the melting of the PCL and PEO lamellae may undergo different pathways. The melting of a PCL lamella starts from the defect and proceeds to the other parts. However, the thickening of the PEO lamellae either in the matrix or in the domains indicates that the reorganization occurred during the heating.

#### Acknowledgements

This work was supported by the Outstanding Youth Fund and the National Science Foundation of China (Grant Nos. 20574083, 50521302, 20174049 and 20131160730). A.-C.S. acknowledges the support from the Natural Science and Engineering Research Council (NSERC) of Canada.

#### References

- [1] Paul DR, Bucknall CB, editors. Polymer blends. Formulation, vol. 1. New York: Wiley; 2000.
- [2] Paul DR, Bucknall CB, editors. Polymer blends. Performance, vol. 2. New York: Wiley; 2000.
- [3] Shonaike GO, Simon GP, editors. Polymer blends and alloys. New York: Marcel Dekker; 1999.
- [4] Laura M, Lorenzo D. Prog Polym Sci 2003;28:663.
- [5] Qiu ZB, Ikehara T, Nishi T. Macromolecules 2002;35:8251.
- [6] He Y, Zhu B, Kai WH, Inoue Y. Macromolecules 2004;37:3337.
- [7] He Y, Zhu B, Kai WH, Inoue Y. Macromolecules 2004;37:8050.
- [8] Kaito A, Iwakura Y, Hatakeyama K, Li YJ. Macromolecules 2007;40:2751.
- [9] Zhang JM, Sato H, Furukawa T, Tsuji H, Noda I, Ozaki Y. J Phys Chem B 2006;110:24463.
- [10] Kaito A. Polymer 2006;47:3548.
- [11] Basire C, Ivanov DA. Phys Rev Lett 2000;85:5587.
- [12] Kyu T, Chiu HW, Guenther AJ, Okabe Y, Saito H, Inoue T. Phys Rev Lett 1999;83:2749.
- [13] Zhang Newby B, Composto RJ. Phys Rev Lett 2001;87:98302.
- [14] Böltau M, Walheim S, Mlynek J, Krausch G, Steiner U. Nature 1998;391:877.
- [15] Voit A, Krekhov A, Enge W, Kramer L, Köhler W. Phys Rev Lett 2005;94:214501.
- [16] Kotnis MA, Muthukumar M. Macromolecules 1992;25:1716.
- [17] Panyukov S, Rabin Y. Phys Rev E 2002;65:61803.
- [18] Arnal ML, Matos ME, Morales RA, Santana OO, Müller A. J Macromol Chem Phys 1998;199:2275.
- [19] Arnal ML, Müller AJ, Maiti P, Hikosaka M. Macromol Chem Phys 2000;201:2493.
- [20] Arnal ML, Müller AJ. Macromol Chem Phys 1999;200:2559.
- [21] Loo YL, Register RA, Ryan AJ. Phys Rev Lett 2000;84:4120.
- [22] Lescanec RL, Muthukumar M. Macromolecules 1993;26:3908.
- [23] Lodge TP, Muthukumar M. J Phys Chem 1996;100:13275.
- [24] Zhu L, Calhoun BH, Ge Q, Quirk RP, Cheng SZD, Thomas BL, et al. Macromolecules 2001;34:1244.
- [25] Zhu L, Huang P, Chen WY, Ge Q, Quirk RP, Cheng SZD, et al. Macromolecules 2002;35:3553.
- [26] Reiter G, Castelein G, Sommer JU, Röttele A, Thurn-Albrecht T. Phys Rev Lett 2001;87:226101.
- [27] Reiter G, Castelein G, Hoerner P, Riess G, Blumen A, Sommer JU. Phys Rev Lett 1999;83:3844.
- [28] Müller AJ, Balsamo V, Arnal ML. Adv Polym Sci 2005;190:1.

- [29] Ashok B, Muthukumar M, Russell TP. *J Chem Phys* 2001;115:1559.
- [30] Massa MV, Dalnoki-Veress K. *Phys Rev Lett* 2004;92:255509.
- [31] Frank CW, Rao V, Despotopoulou MM, Pease RFW, Hinsberg WD, Miller RD, et al. *Science* 1996;273:912.
- [32] Despotopoulou MM, Frank CW, Miller RD, Rabolt JF. *Macromolecules* 1996;29:5797.
- [33] Sommer JU, Reiter G. *J Chem Phys* 2000;112:4384.
- [34] Reiter G, Sommer JU. *Phys Rev Lett* 1998;80:3771.
- [35] Reiter G, Sommer JU. *J Chem Phys* 2000;112:4376.
- [36] Jiang Y, Jin XG, Han CC, Li L, Wang Y, Chan CM. *Langmuir* 2003;19:8010.
- [37] Jiang Y, Yan DD, Gao X, Han CC, Jin XG, Li L, et al. *Macromolecules* 2003;36:3652.
- [38] Chuang WT, Jeng US, Sheu HS, Hong PD. *Macromol Res* 2006;14:45.
- [39] Chuang WT, Shih KS, Hong PD. *J Polym Res* 2005;12:197.
- [40] Chuang WT, Jeng US, Hong PD, Sheu HS, Lai YH, Shih KS. *Polymer* 2007;48:2919.
- [41] Qiu ZB, Ikehara T, Nishi T. *Polymer* 2003;44:3101.
- [42] Chen EQ, Jing AJ, Weng X, Huang P, Lee SW, Hsiao BS, et al. *Polymer* 2003;44:6051.
- [43] Cheng SZD, Zhang AQ, Barley JS, Chen JH, Habenschuss A, Zschack PR. *Macromolecules* 1991;24:3937.
- [44] Cheng SZD, Chen JH, Barley JS, Zhang AQ, Habenschuss A, Zschack PR. *Macromolecules* 1992;25:1453.